Histol Histopathol (2011) 26: 1531-1543

http://www.hh.um.es

Histology and Histopathology

Cellular and Molecular Biology

PTPIP51, a positive modulator of the MAPK/Erk pathway, is upregulated in glioblastoma and interacts with 14-3-3ß and PTP1B *in situ*

M.K. Petri[1], P. Koch[1], A. Stenzinger[2], K. Kuchelmeister[3], U. Nestler[4], A. Paradowska[5], K. Steger[5], A. Brobeil[1], M. Viard[1] and M. Wimmer[1]

[1]Institute of Anatomy and Cell Biology, Justus-Liebig-University, Giessen, Germany, [2]Institute of Pathology, University Hospital Heidelberg, Heidelberg, Germany, [3]Institute of Neuropathology, University Hospital Bonn, Bonn, Germany, [4]Department of Neurosurgery, Justus-Liebig-University, Giessen, Germany and [5]Department of Urology and Pediatric Urology, Justus-Liebig-University, Giessen, Germany

Summary. Glioblastoma multiforme (GBM) is the most common and most malignant primary brain tumour. Protein tyrosine phosphatase interacting protein 51 (PTPIP51) is an interaction partner of 14-3-3ß, which correlates with the grade of malignancy in gliomas. In this study PTPIP51 and its interacting partners 14-3-3ß, PTP1B, c-Src, Raf-1 as well as EGFR were investigated in human glioblastoma.

Twenty glioblastoma samples were analyzed on transcriptional and translational level by immunohistochemistry, *in situ* hybridization and RT-PCR. To compare PTPIP51 expression in gliomas of different malignancies, quantitative RT-PCR for grade II astrocytoma and GBM samples was employed. Additionally, we analyzed the correlation between PTPIP51 and 14-3-3ß transcription, and checked for *in situ* interaction between PTPIP51 and 14-3-3ß and PTP1B, respectively.

PTPIP51 and 14-3-3ß mRNA showed a tumour grade dependent upregulation in gliomas. Glioblastoma cells displayed a strong immunoreaction of PTPIP51, which co-localized with 14-3-3ß and PTP1B. The duolink proximity ligation assay corroborated a direct *in situ* interaction of PTPIP51 with both proteins, known to interact with PTPIP51 *in vitro*. The *in vitro* interacting partners Raf-1 and c-Src showed a partial co-localization. Besides, immune cells located in capillaries or infiltrating the tumour tissue and endothelial cells of pseudoglomerular vessels revealed a high PTPIP51 expression.

The upregulation of PTPIP51 and its connection with the EGFR/MAPK pathway by 14-3-3ß via Raf-1 and by PTP1B via c-Src, argue for a functional role of PTPIP51 in the pathogenesis of human glioblastoma.

Key words: Glioblastoma, PTPIP51, 14-3-3ß, EGFR, MAPK, Raf-1, Glioma

Offprint requests to: Meike Katinka Petri, Institute of Anatomy and Cell Biology, Justus-Liebig-University Giessen, 35385 Giessen, Germany. e-mail: meike.petri@anatomie.med.uni-giessen.de

Introduction

The incidence of gliomas is increasing worldwide. 18,820 new cases of human primary central nervous system tumours are diagnosed annually in the United States of America, about 60% are gliomas and 30-40% of these account for glioblastoma (GBM) (Khan et al., 2009). GBM is the most frequent and most malignant form of neuroepithelial tumour. The mean survival time of GBM patients is still around one year, despite significant advances in therapeutic options (McLendon et al., 2007).

PTPIP51 is a novel protein that has been shown to be expressed in many human cancers (Lv et al., 2006; Stenzinger et al., 2009). As demonstrated by Koch et al. (2008, 2009b) PTPIP51 is expressed in human keratinocyte carcinomas and prostate cancer. Comparing benign prostate hyperplasia with prostate carcinoma provided evidence that PTPIP51 expression is partially controlled by promoter methylation. Lv et al. (2006) demonstrated PTPIP51 mRNA-expression in various carcinomas.

PTPIP51 is evolutionary conserved and was shown to interact *in vitro* with the non-transmembrane protein-tyrosine phosphatase, Protein Tyrosine Phosphatase 1B

(PTP1B) (Stenzinger et al., 2005, 2009). The protein is phosphorylated *in vitro* and *in situ* at Tyr176 by Src kinase and dephosphorylated by PTP1B (Stenzinger et al., 2009). In HEK 293 and HeLa cells, PTPIP51 overexpression was shown to enhance apoptosis (Lv et al., 2006).

Recently, two independent studies by Jin et al. (2004) and Ewing et al. (2007) demonstrated the interaction between the two isoforms 14-3-3ß, 14-3-3γ and PTPIP51. The study of Yang et al. (2009) demonstrated a correlation between the grade of malignancy and the expression of 14-3-3ß and 14-3-3η in gliomas. In contrast, normal brain tissue was not found to express these two 14-3-3 isoforms. The isoforms ß and η belong to a superfamily of 14-3-3 proteins, which are differentially expressed in many human tissues. 14-3-3 proteins have been implicated in numerous cellular processes, such as tumourigenesis, cell cycle control and apoptosis (Cao et al., 2008).

Yu and co-workers (2008) reported PTPIP51 to interact with Raf-1 through 14-3-3 protein, thereby modulating cellular motility and morphology by the mitogen activated protein kinase (MAPK) cascade. The MAPK/Erk pathway is involved in a variety of cellular functions such as growth, proliferation, differentiation, migration and apoptosis. This pathway has been extensively studied in glioblastoma cells (Lopez-Gines et al., 2008). The data available so far consider PTPIP51 to play a role in cellular differentiation, motility, cytoskeleton formation and apoptosis.

This study primarily aimed to investigate the PTPIP51-expression profile in GBM, applying RT-PCR, quantitative real time PCR, *in situ* hybridization and immunohistochemistry. Moreover, cell specific co-expression of the proteins 14-3-3ß, Raf-1, PTP1B, c-Src and EGFR were assessed at the mRNA and protein level. Furthermore, the direct interaction of PTPIP51 with 14-3-3ß and PTP1B *in situ* was substantiated.

An earlier study by Koch et al. (2009a) displayed the expression of PTPIP51 to be restricted to neurons in specific areas of normal mouse brain and glial cells did not show an expression of PTPIP51.

Data obtained in the present study will set the base for further studies that aim to investigate the putative role of PTPIP51 in glioblastoma formation.

Material and methods

Samples of twenty glioblastoma cases and samples of four astrocytomas were included in this study (Table 1).

Glioblastoma specimens were stained immunohistochemically for PTPIP51, 14-3-3ß, c-Src, Raf-1, PTP1B, EGFR, apoptosis (TUNEL) and proliferation (Ki67). The cell specific expression of PTPIP51 was corroborated by means of *in situ* hybridization.

Four intraoperatively obtained tissue samples of primary glioblastoma and one of recurrent glioblastoma were examined for mRNA expression of PTPIP51, 14-3-3ß, c-Src, Raf-1 and PTP1B. Moreover, to obtain quantitative data on the transcriptional activity of the 14-3-3ß and PTPIP51 gene in grade II astrocytoma (n=4 paraffin embedded samples) and glioblastoma (n=5 paraffin embedded samples) kinetic PCR was employed.

Immunohistochemistry

The tumour tissue was fixed in neutral-buffered formalin for 48h, embedded in paraffin, sectioned and stained with H&E. The samples were categorized according to the WHO classification and diagnosed as GBM.

Paraffin samples were obtained from the Institute of Neuropathology, University Hospital Bonn. The patients had given informed consent that parts of the histological specimens can be used for research purposes. The sections were deparaffinized in xylene and rehydrated in graded ethanol. Prior to the staining procedure, antigen retrieval using microwave-oven heating (2x5min, 800W) in 10mM standard sodium citrate buffer (pH 6.0) was carried out for all antibodies used in this study.

Nonspecific binding sites were blocked with phosphate-buffered saline (PBS) containing 5% bovine serum albumin and 5% normal goat serum. Immunoreaction with the primary antibodies (Table 2) was performed overnight at room temperature, followed by incubation with the appropriate secondary antibodies

Table 1. Tumour specimens included in the study Tumours.

	Age (years)	Sex	Localization	Tumour specimens	WHO-Grade
1	65	M	central, left	GBM	IV
2	63	F	frontal, right	GBM	IV
3	78	F	frontal, right	GBM	IV
4	72	M	fronto-temporal, left	GBM	IV
5	76	M	temporal, right	GBM	IV
6	70	M	central, right	GBM	IV
7	60	M	temporal, right	GBM	IV
8	66	M	temporo-dorsal, left	GBM	IV
9	72	F	temporo-medial, right	GBM	IV
10	61	M	temporo-parietal, left	GBM	IV
11	42	M	central, left	GBM	IV
12	67	M	frontal, right	GBM	IV
13	78	M	central, right	GBM	IV
14	68	F	temporo-polar, left	GBM	IV
15	52	M	precentral/central, left	GBM	IV
16	33	M	temporo-medial, right	Astrocytoma	II
17	23	F	insula, left	Astrocytoma	II
18	44	F	corpus callosum, left	Astrocytoma	II
19	31	M	insula, right	Astrocytoma	II
20	55	M	occipital, left (hemianopsia)	GBM magnocellular	IV
21	55	F	parietal, right	GBM	IV
22	46	M	parietal/pre-central gyrus, left	GBM, relapse	IV
23	66	M	parietal, occipital right	GBM, relapse	IV
24	76	M	Broca region, left	GBM	IV

No. 1-19 were analyzed by immunocytochemistry and No. 11-19 by quantitative real time PCR. Tumours No. 20-24 were analyzed by reverse transcriptase PCR.

(Table 2) for 1 h at room temperature. Subsequently, the slides were coverslipped in carbonate buffered glycerol at pH 8.6.

The polyclonal antibody against PTPIP51 was raised as described and characterized in previous studies (Koch et al., 2009a).

Primary antibodies were visualized by Alexa fluor 488 and Alexa fluor 555 secondary antibodies. For each series of antibody staining sections were incubated with medium lacking PTPIP51 antibody, serving as an internal negative control. Nuclei were displayed by DAPI.

Apoptosis was detected using the *in situ* cell death detection kit ApopTag (Chemicon International, USA # S7110) which employs an indirect TUNEL method, utilizing an anti-digoxigenin antibody that is conjugated to a fluorescein reporter molecule. It provides indirect immunofluorescence staining. Results were analyzed by using fluorescence microscopy. The kit was used according to the instructions by the manufacturer.

Immunofluorescence analysis and photo-documentation were performed on an Axioplan 2 fluorescence microscope equipped with Plan-Apochromat objectives (Carl Zeiss Jena, Germany). Visualization of the secondary antibody Alexa fluor 555 was achieved with an excitation filter of 530-560 nm and an emission filter with a range 572.5-647 nm. Alexa Fluor 488 was visualized by an excitation filter with 460-500nm and an emission filter 512-542 nm.

Duolink proximity ligation assay (DPLA)

Interaction of PTPIP51 with either PTP1B or 14-3-3ß was detected by the proximity ligation assay kit DuoLink (Olink biosciences, Uppsala, Sweden, PLA probe anti-rabbit minus for the detection of the rabbit PTPIP51 antibody, Cat.# 90602; PLA probe anti-mouse plus for the detection of the mouse anti PTP1B or 14-3-3ß antibody, Cat.# 90701; Detection Kit 563, Cat.# 90134). The DuoLink proximity ligation assay secondary antibodies only hybridise when the two different PLA probes (probe anti-rabbit minus and probe anti-mouse plus) have bound to proteins in proximity closer than 40 nm. This proximity results in ligation forming a circular template and amplification step the fluorophore coupled testing probe binds the amplified oligonucleotide strands. Addition of the fluorescent labelled oligonucleotides that hybridize to the rolling circle amplification (RCA) product leads to a point-shaped signal that is visible in fluorescence microscopy.

Methanol-fixed air-dried samples were per-incubated with blocking agent for 1h. After washing in PBS for 10 min, primary antibodies for PTPIP51 and PTP1B, or PTPIP51 and 14-3-3ß were applied to the samples. The antibodies were diluted in the blocking agent at a concentration of 1:500 and 1:100, respectively.

Table 2. List of the antibodies used in this study.

	Immunogen	Antibody Source	Clone	Dilution	Manufacturer
PTPIP51	Human recombinant PTPIP 51 protein encoding amino acids (aa) 131-470	Rabbit polyclonal		1:400	Prof. HW Hofer, Biochemical Department, University Konstanz, Germany
14-3-3 ß	Epitope mapping the C-terminus of human origin	Mouse monoclonal	A-6	1:100	Santa Cruz Cat# sc-25276
PTP1B	Human recombinant protein tyrosine phosphatase 1B (aa 1 – 321)	Mouse monoclonal	107AT531	1:100	Abgent Cat#AM8411
Glial fibrillary acidic protein	Purified porcine glial filament from spinal cord	Mouse monoclonal	GA5	1:200	Chemicon Cat# MAB3402
Raf-1	Epitope mapping the C-terminus of human origin	Mouse monoclonal	E-10	1:50	Santa Cruz Cat# sc-7267
c-Src	Full-length human recombinant c-Src	Mouse monoclonal	17AT28	1:100	Santa Cruz Cat# sc-130124
EGFR	Plasma membranes of A431 cells	Mouse monoclonal	2E9	1:75	Santa Cruz Cat# sc-57091
Ki67	Human recombinant peptide corresponding to a 1002 bp Ki-67 cDNA fragment	Mouse monoclonal	MIB-1	1:100	Dako Cytomation Cat# M 7240
CD20	CD20 protein	Mouse monoclonal	B9E9	1:100	Thermo Scientific Cat # MA1-7634
CD34	CD34 protein from human endothelial vesicles	Mouse monoclonal	QBEND-10	1:100	ThermoScientific Cat.# Ma35170
Granulocyte marker SPM250	nuclei from Pokeweed nitrogen-stimulated human peripheral blood lymphocytes	Mouse monoclonal	his48	1:100	Santa Cruz Cat# sc-65523
α-smooth muscle actin- FITC antibody	N-terminal synthetic decapeptide of α-smooth muscle actin	Mouse monoclonal	clone 1A4	1:100	SigmaAldrich Cat# F3777
Alexa fluor 555 Coupled to anti-rabbit antibody	IgG heavy chains from rabbit	Goat		1:800	Invitrogen Cat# A21428
Alexa fluor 488 Coupled to anti-mouse antibody	IgG heavy chains from mouse	Goat		1:800	Invitrogen Cat# A11029
ApopTag® Fluorescein *In Situ* Apoptosis Detection Kit					Chemicon International S7107

Incubation was done overnight in a pre-heated humidity chamber. Slides were washed three times in PBS for 10 min. Duolink PLA probes detecting rabbit or mouse antibodies were diluted in the blocking agent at a concentration of 1:5 and applied to the slides following incubation for 2h in a pre-heated humidity chamber at 37°C. Washing three times in PBS for 10 min removed unbound PLA probes. For hybridization of the two Duolink PLA probes Duolink Hybridization stock was diluted 1:5 in high purity water and slides were incubated in a pre-heated humidity chamber for 15 min at 37°C. The slides were washed in TBS-T for 1 min under gentle agitation. The samples were incubated in the ligation solution consisting of Duolink Ligation stock (1:5) and Duolink Ligase (1:40) diluted in high purity water for 90 min at 37°C. Detection of the amplified probe was done with the Duolink Detection kit. Duolink Detection stock was diluted 1:5 in high purity water and applied for 1 h at 37°C. Final washing steps were done by SCC buffer and 70% ethanol.

H&E

The histomorphological characteristics were evaluated by hematoxylin and eosin staining.

In situ hybridization

In situ hybridization was performed as described previously (Koch et al., 2009a).

Reverse transcriptase-polymerase chain reaction (RT-PCR)

For assessment of RT-PCR five glioblastoma tissue specimens were obtained during neurosurgical resection. The tissue samples were immediately transferred into RNA-later (Qiagen, Hilden, Germany) and stored deep frozen at -20°C according to the manufacturer's instructions. All tissue samples used for RT-PCR were obtained from the Department of Neurosurgery, Justus-Liebig-University, Giessen. Prior to resection, patients had given informed consent to using parts of the histological specimen for research purposes.

The RNA extraction was performed using the RNA extraction kit RNeasy MINI (Qiagen, Hilden, Germany) according to the manufacturer's instructions.

Qualitative reverse transcriptase PCR was performed on an iCycler using SYBR Green Supermix (BioRad, Munich, Germany) to visualize the respective amplicons. 2 μl cDNA were used per sample. Cycling conditions were 94°C for 2 min, followed by 40 cycles of 94°C (PTPIP51); 58°C (PTP1B); 63°C (c-Src); 63.5°C (Raf-1) and 60°C (14-3-3ß) for 30 sec, 55°C for 30 sec and 72°C for 2 min. The primers were employed for PTPIP51, PTP1B, c-Src, Raf-1 and 14-3-3ß (Table 3).

PCR products were visualized by agarose gel electrophoresis. While amplification of a 90 bp ß-actin

Table 3. Primer used for RT-PCR and for quantitative real time PCR.

	Primer RT-PCR (fresh tissue specimen)	size	template
PTPIP51	forward 5´-GCAGGTGGTGCTATCAGGTC-3´ reverse 5'-AGCTCCAGGGCCAACTTCATC-3'	232 BP	1294-1525
PTP1B	forward 5'-GGAGATGGAAAAGGAGTTC-3' reverse 5'-TGCTTTTCTGCTCCCACAC-3'	311 BP	177-487
14-3-3ß	forward 5'-ATTCGTCTTGGTCTGGCACT-3' reverse 5'-CAGGCTACAGGCCTTTTCAG-3'.	78 BP	689-766, 784-861
c-Src	forward 5'-ATGGTGAACCGCGAGGTGCT-3' reverse 5'-GATCCAAGCCGAGAAGCCGGTCTG-3'	244 BP	1753-1996
Raf-1	forward 5'-CAGCCCTGTCCAGTAGC-3' reverse 5'-GCCTGACTTTACTGTTGC-3'	614 BP	1287-1900
ß-actin	forward 5'-TTCCTTCCTGGGCATGGAGT-3' reverse 5'-TACAGGTCTTTGCGGATGTC-3'	90 BP	2439-2528
	Primer quantitative RT-PCR (paraffin embedded tissue)		
PTPIP51	forward 5'-TCAAGGAGCATGTGGACAAA-3' reverse 5'-ATAGCACCACCTGCCAAGAA-3'	80 BP	1228-1307
14-3-3ß	forward 5'-ATTCGTCTTGGTCTGGCACT-3' reverse 5'-CAGGCTACAGGCCTTTTCAG-3'.	78 BP	689-766, 784-861
ß-actin	forward 5'-TTCCTTCCTGGGCATGGAGT-3' reverse 5'-TACAGGTCTTTGCGGATGTC-3'	90 BP	2439-2528
GAPDH	forward 5'-ATGCCAGTGAGCTTCCCGTTCA-3' reverse 5'-TGGTATCGTGGAAGGACTCATGA-3'	189 BP	628-794

product served as positive control, negative controls included samples lacking reverse transcriptase.

Quantitative real time PCR

Five paraffin-embedded GBM tissues and four samples from patients with grade II astrocytoma were used for quantification of mRNA. The purification of RNA was done using the QIAamp DNA FFPE tissue kit (Qiagen, Hilden, Germany) according to the manufacturer's instruction.

The amplification of cDNA was carried out in 25 μl reaction volume on the iCycler iQ Real-Time PCR Detection System (Bio Rad, Munich, Germany). The final reaction tubes contained 100nM as PTPIP51, 14-3-3ß and reference genes ß-actin and GAPDH (Table 3), 12.5 μl iQ SYBR Green Supermix (Bio Rad) and 2 μl of DNA template. The PCR conditions were 94°C for 3 min followed by 40 cycles for 30 sec, 60°C for 30 sec and 72°C for 1min. Melting curves were generated for both genes after amplification. Negative controls were included in each run. The selection of appropriate combination of reference genes for expression analysis of PTPIP51 in GBM and astrocytoma II tissue was carried out using NormFinder Program. PCR-products were additionally electrophoresed on a 3% agarose gel and visualized by GelRed reagent.

Results

This study demonstrates for the first time the cell-specific expression of PTPIP51 mRNA and protein in human glioblastoma. Immunohistochemical experiments and *in situ* hybridization revealed a strong expression of PTPIP51 in GBM tumour cells and endothelial cells and immune cells. Additionally, the PTPIP51 expression profile was assayed in apoptosis by TUNEL and in proliferation with Ki67 by double immunostaining. Furthermore, we explored the interacting partners of PTPIP51, 14-3-3ß, Raf-1, PTP1B, c-Src and EGFR. The transcription of the respective signalling partners was shown by qualitative reverse transcriptase PCR. The correlation of the tumour grade of gliomas with the quantitative expression of both, PTPIP51 and 14-3-3ß, was examined by quantitative real time PCR comparing GBM and grade II astrocytoma.

In situ expression profile of PTPIP51 mRNA and protein

Immunohistochemical staining of 15 GBM samples revealed PTPIP51 protein expression in tumour cells as identified by subsequent H&E staining of the sections (Fig. 1A-C). Probing glioblastoma samples with both PTPIP51 antibody and GFAP antibody confirmed the expression of PTPIP51 in malignant glial cells (Fig. 1D-

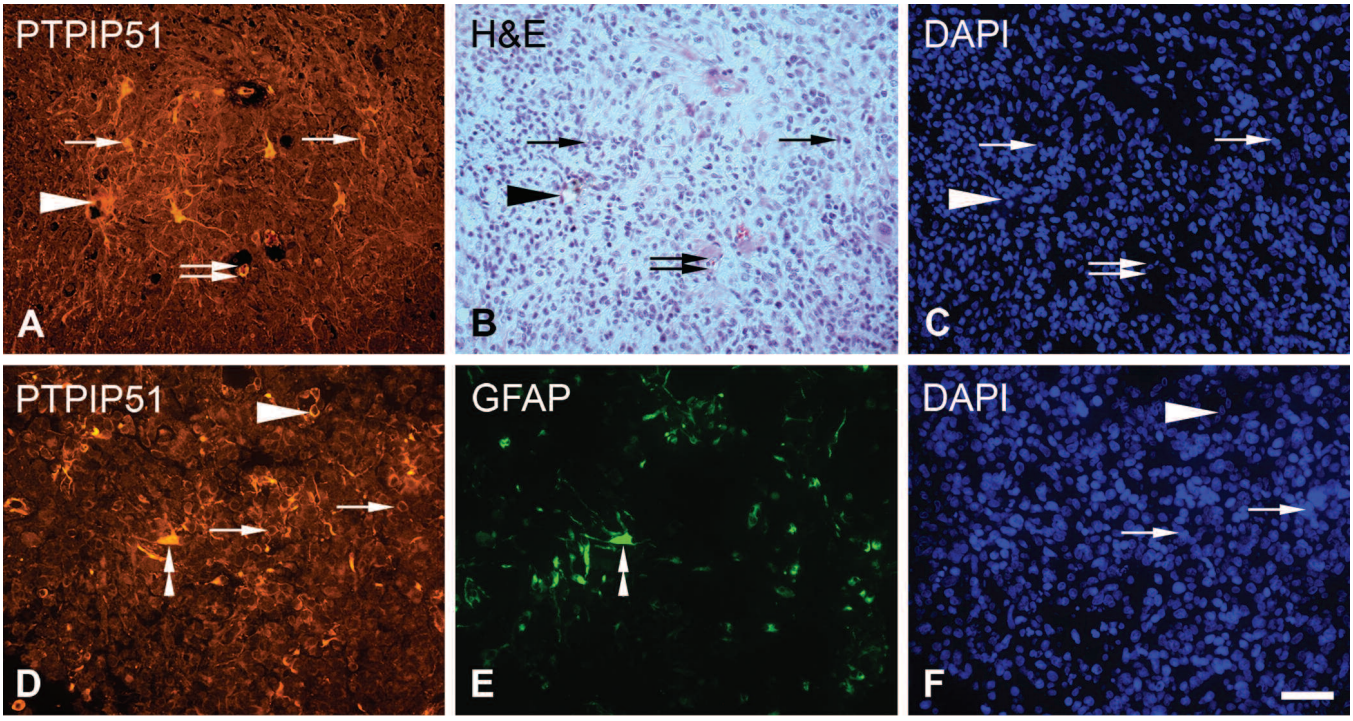

Fig. 1. Immunostaining of PTPIP51 in sections of human glioblastoma. **A.** PTPIP51 immunostaining. **B.** H&E staining of section A. **C.** DAPI staining of section A. **D.** PTPIP51 immunostaining. **E.** GFAP staining of section D. **F.** DAPI staining of section D. Arrows: PTPIP51 positive glioblastoma cells, arrowheads: PTPIP51 positive endothelial cells, double arrowheads: PTPIP51 and GFAP positive reactive astrocyte, double arrow: PTPIP51 positive immune cell (neutrophil granulocyte). Bar: 50 μm.

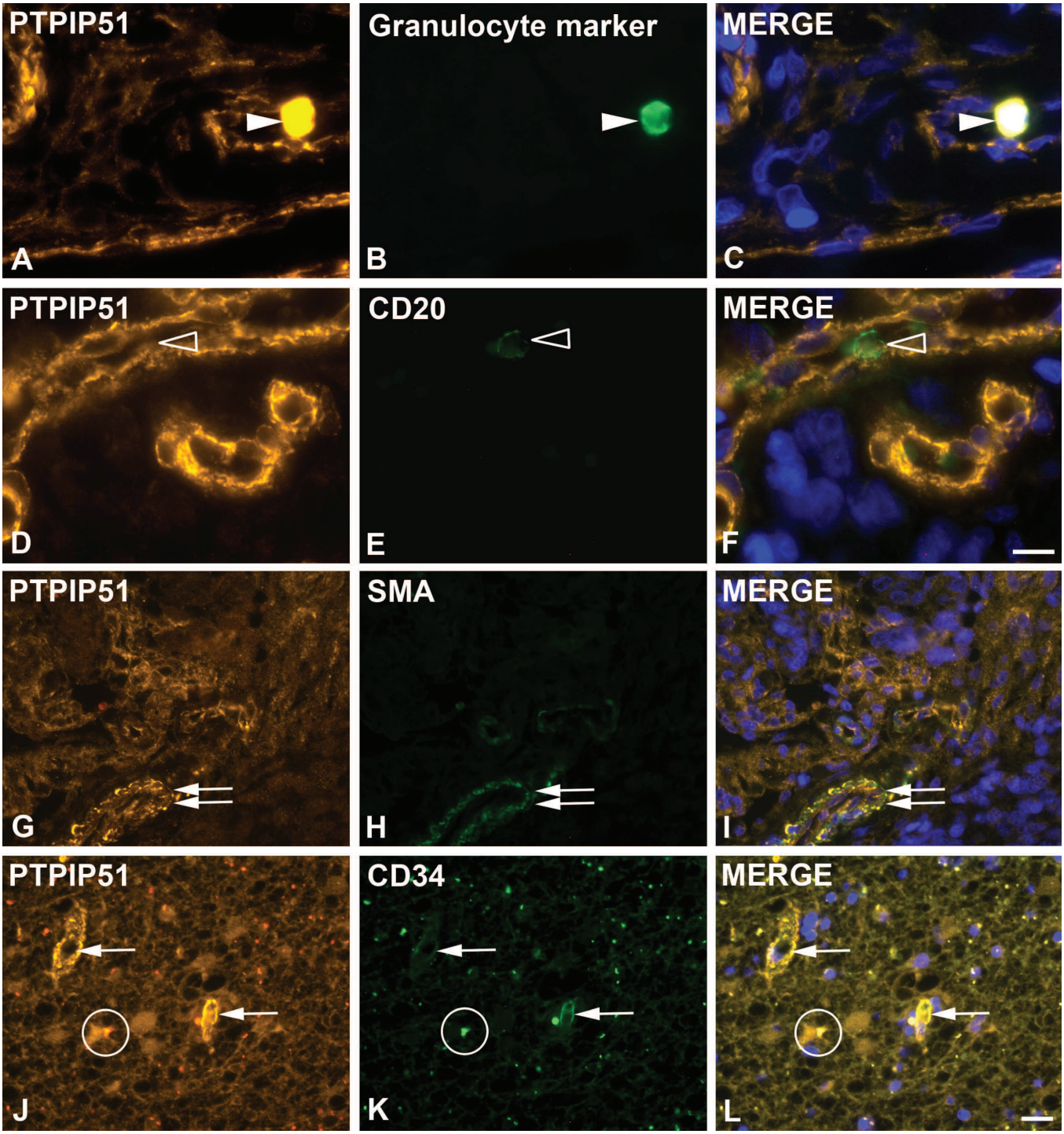

Fig. 2. PTPIP51 expression in immune cells, smooth muscle cells and endothelial cells. **A.** PTPIP51 immunostaining. **B.** granulocyte marker of section A. **C.** Merge of A, B and DAPI. **D.** PTPIP51 immunostaining. **E.** B lymphocyte in section D detected by CD20. **F.** Merge of D, E and DAPI. **G.** PTPIP51 immunostaining. **H.** α-sma of section G. **I.** Merge of G,H and DAPI. **J.** PTPIP51 immunostaining. **K.** Endothelial cells detected by CD34 in section J. **L.** Merge of J, K and DAPI. Arrowhead: neutrophil granulocytes; blank arrowhead: B lymphocytes; double arrow: smooth muscle cells; arrow: endothelial cells; white circle: lipofuscin granula . Bars: A-F, 10 μm; G-L, 20 μm.

F). Endothelial cells (Fig. 2J-L), smooth muscle cells (Fig. 2G-I) and immune cells also showed PTPIP51 expression. In endothelial cells of normal and of pseudoglomerular vessels PTPIP51 protein was restricted to the plasmamembrane and to the nucleus. Granulocytes located in capillary lumina or infiltrating the tumour, as well as the necrotic tissue, displayed a strong PTPIP51 immunoreaction (Fig. 2A-C). In contrast to granulocytes, B lymphocytes did not show any PTPIP51 expression (Fig. 2D-F).

Matching the protein expression profile, PTPIP51 mRNA was found in the cytoplasm of tumour cells and in the cytoplasm of endothelial cells as detected by *in situ* hybridization (Fig. 3).

In situ expression profile of PTPIP51 and its interacting partners

PTPIP51 and 14-3-3ß showed a strict co-localization. Both proteins were found in glioblastoma cells, endothelial cells and in immune cells. The glioblastoma cells displayed a strong cytoplasmic reaction (Fig. 4A-C). In astrocytoma, a co-localization for PTPIP51 and 14-3-3ß was seen, but to a much lower extent (Fig. 4D-F).

To corroborate the interaction of PTPIP51 and 14-3-3ß, a duolink proximity ligation assay was applied to GBM and astrocytoma sections. In all investigated samples, hybridized and amplified antibody-linked

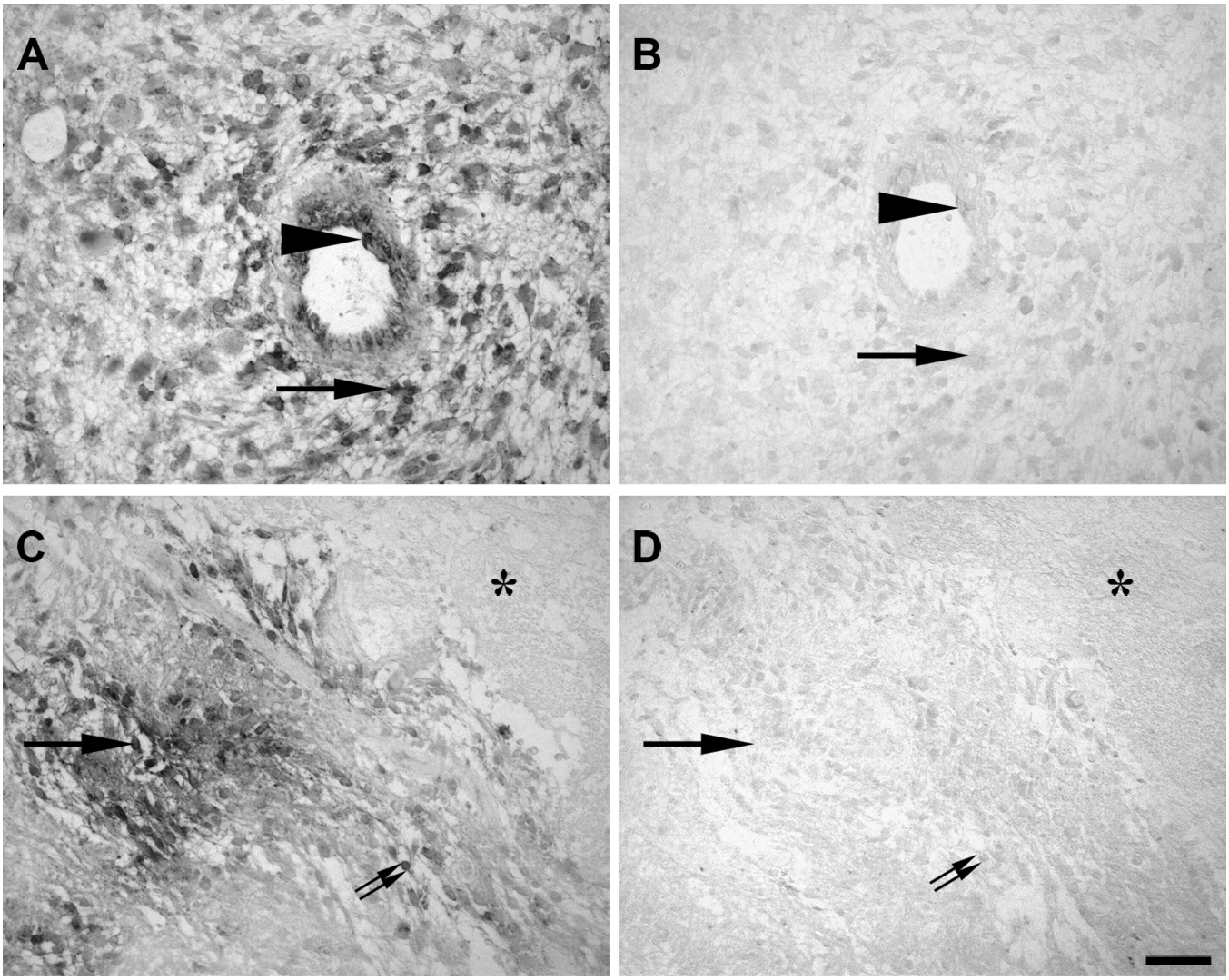

Fig. 3. *In situ* hybridization of PTPIP51 in sections of human glioblastoma. **A.** Anti-sense probe. **B.** Sense probe of parallel section to A. **C.** Anti-sense probe. **D.** Sense probe in parallel section to C. Arrows: PTPIP51 mRNA in glioblastoma cells, arrowhead: PTPIP51 mRNA in endothelial cells, double arrow: immune cells, asterisk: necrotic tissue. Bar: 50 μm.

nucleotide strands were detected. Every dot corresponds to an interaction between PTPIP51 and 14-3-3ß.

As seen in Figure 4G and H, glioblastoma and astrocytoma cells displayed hybridized and amplified antibody-linked nucleotide strands, revealing the *in situ* interaction between PTPIP51 and 14-3-3ß.

GBM tumour cells situated around pseudoglomerular vessels, as well as endothelial cells and immune cells, displayed a co-localization of PTPIP51 with PTP1B (Fig. 5A-C). To confirm an *in situ* interaction of PTPIP51 and PTP1B, a duolink proximity ligation assay was performed. As seen in Figure 5D glioblastoma cells displayed hybridized and amplified antibody-linked nucleotid strands, revealing the interaction between PTPIP51 and PTP1B.

Raf-1 and PTPIP51 displayed a strong co-localization in the vessels surrounding tumour cells (Fig. 6A-C).

There was only a partial co-localization of PTPIP51 and c-Src (Fig. 6D-F). In contrast to high PTPIP51 expression in the cytoplasm of tumour and immune cells c-Src is only present in some of these cells.

A majority of tumour cells displayed a co-localization of PTPIP51 and EGFR (data not shown).

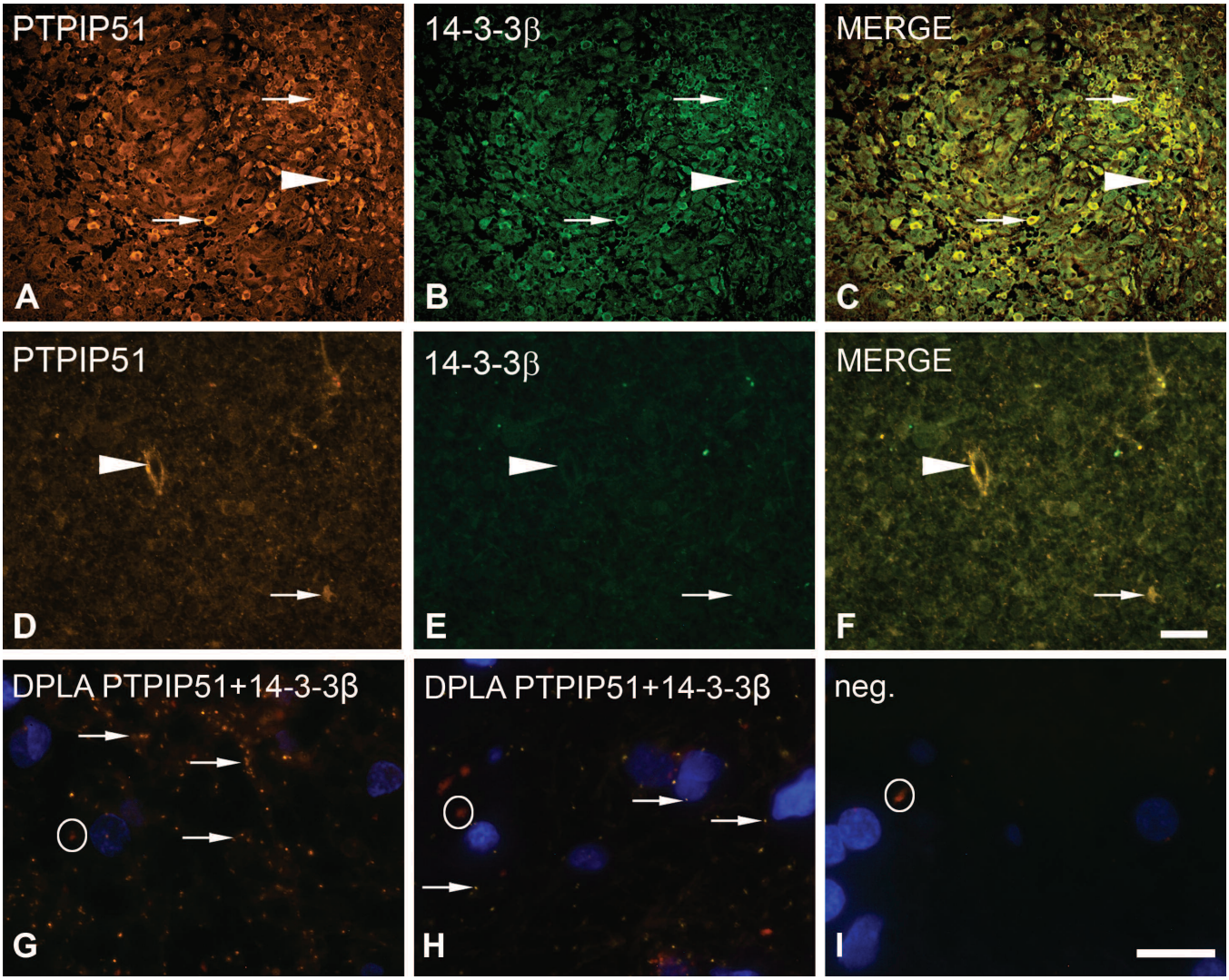

Fig. 4. PTPIP51 and its interacting partner 14-3-3ß - *in situ* co-localization analysis and Duolink proximity ligation assay in sections of human glioblastoma and astrocytoma. **A.** PTPIP51 immunostaining GBM. **B.** 14-3-3ß immunostaining of section A. **C.** Merge of A and B. **D.** PTPIP51 immunostaining astrocytoma. **E.** 14-3-3ß immunostaining of section D. **F.** Merge of D and E. Arrows: PTPIP51 positive glioblastoma cells, arrowheads: PTPIP51 positive endothelial cells, double-arrows: immune cells. **G.** GBM duolink proximity ligation assay for PTPIP51 and 14-3-3ß. **H.** astrocytoma duolink proximity ligation assay for PTPIP51 and 14-3-3ß. Interaction of both proteins is seen as orange dots (arrows). **I.** Negative control. White circles: lipofuscin granules. Bars: A-F, 50 μm; G-I, 10 μm.

Stained by Ki-67, proliferating cells showed a strong expression of PTPIP51 in the cytoplasm with elevated concentration near the plasmamembrane (Fig. 7A-C).

TUNEL assay analysis of GBM sections did not show PTPIP51 positive cells executing apoptosis (Fig. 7D-F).

mRNA expression of PTPIP51 and its interaction partners

Qualitative reverse transcriptase PCR analysis: The mRNA expression of PTPIP51 and its *in vitro* interaction partners was tested by reverse transcriptase PCR. As demonstrated in Figure 8, the samples 1, 2, 3 and 5 expressed a considerable amount of PTPIP51, PTP1B, 14-3-3ß, Raf-1 and c-Src. A different expression pattern was observed in sample number 4, which had been obtained from a patient with a recurrent GBM. The histopathological findings of this specimen showed healthy cerebral tissue with only singular tumour cells. In this case attenuated expression of PTPIP51 and PTP1B was found, c-Src was barely detectable, and Raf-1 was lacking (Fig. 8).

Comparison of PTPIP51 expression levels in grade II astrocytoma and glioblastoma by quantitative PCR

PTPIP51 expression levels of 5 GBM and 4 grade II astrocytoma samples were assessed by quantitative PCR. Candidate reference genes for normalization and the best

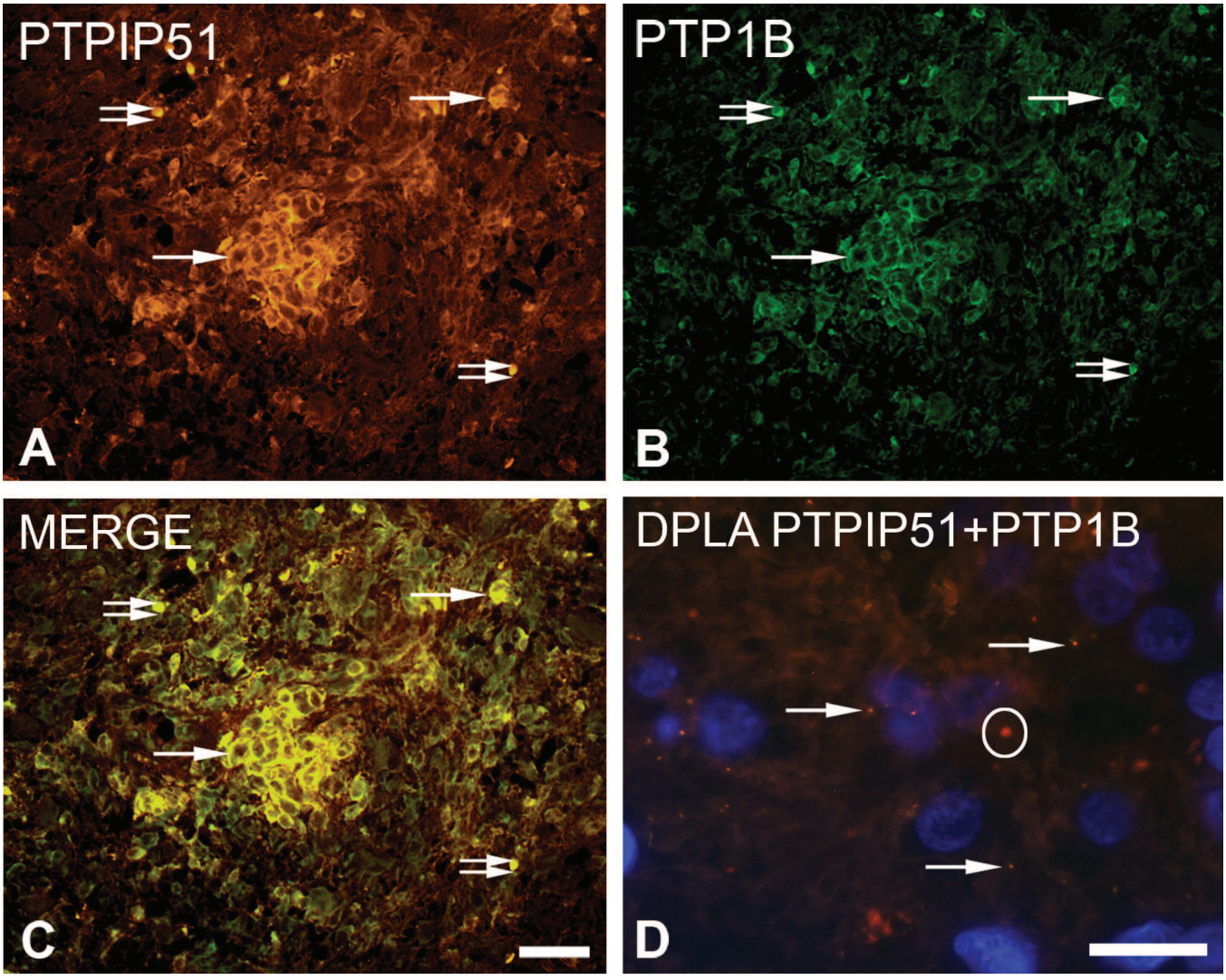

Fig. 5. PTPIP51 and its interacting partner PTP1B in sections of human glioblastoma. **A.** PTPIP51 immunostaining. **B.** PTP1B immunostaining of section A. **C.** Merge of section A and B. Arrows: PTPIP51 positive glioblastoma cells; Double arrows: immune cells. **D.** Duolink proximity ligation assay for PTPIP51 and PTP1B. Interaction of both proteins is seen as orange dots (arrows). Bars: A-C, 20 μm; D, 10 μm.

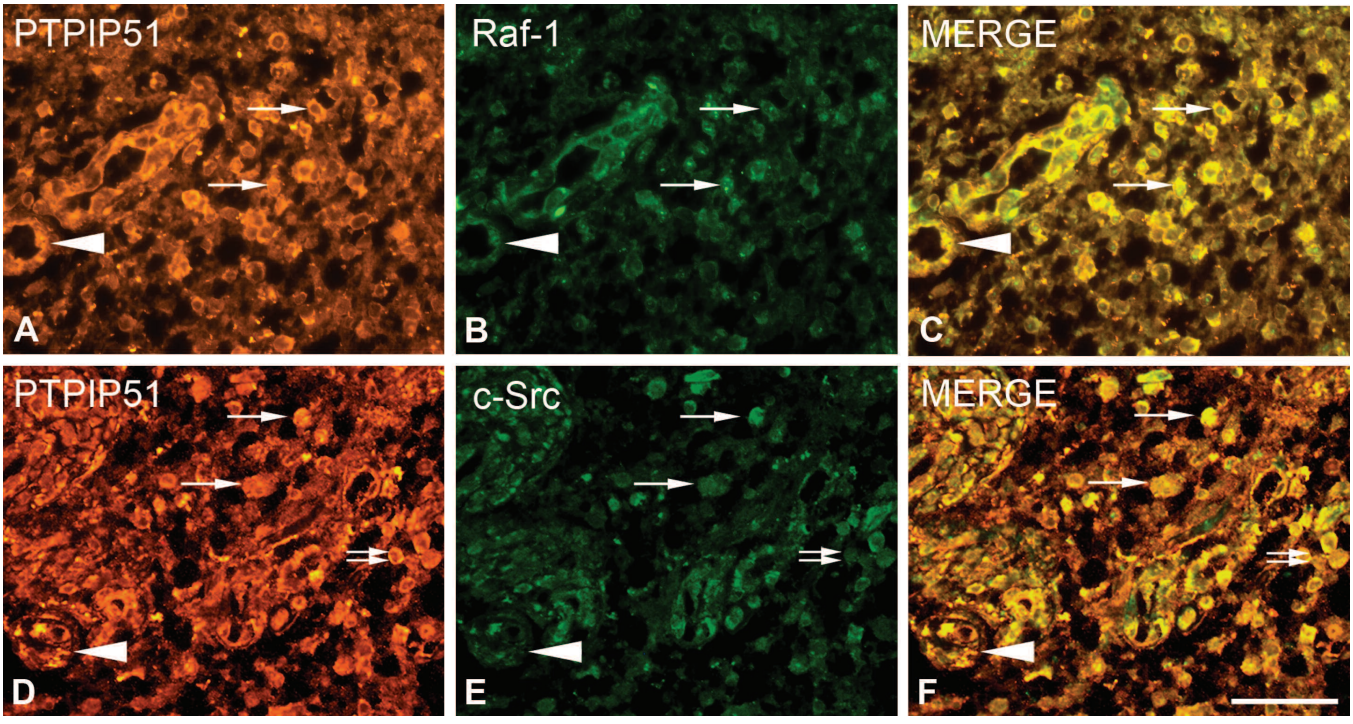

Fig. 6. PTPIP51 and its interacting partners Raf-1 and c-Src in sections of human glioblastoma. **A.** PTPIP51 immunostaining. **B.** Raf-1 immunostaining of section A. **C.** Merge of A and B. **D.** PTPIP51 immunostaining. **E.** c-Src immunostaining of section D. **F.** Merge of D and E. Arrows: PTPIP51 positive glioblastoma cells, arrowheads: PTPIP51 positive endothelial cells, double-arrows: immune cells. Bar: 50 μm.

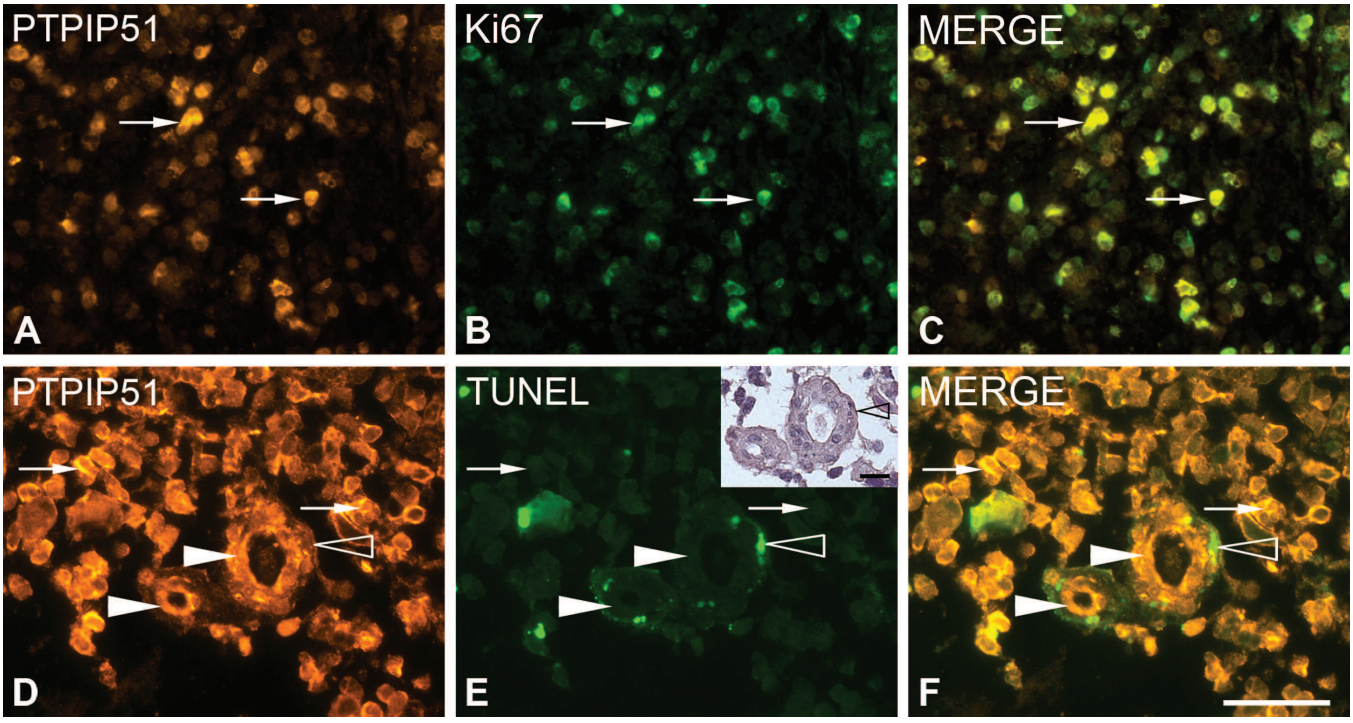

Fig. 7. PTPIP51 protein expression and investigation of proliferation and apoptosis by Ki67 antibody and TUNEL-assay. **A.** PTPIP51 immunostaining. **B.** Ki67 immunostaining of section A. **C.** Merge of A and B. **D.** PTPIP51 immunostaining. **E.** TUNEL-assay of section D, insert: H.E. staining of detail **F.** Merge of D and E. Arrows: PTPIP51 positive glioblastoma cells, arrowheads: PTPIP51 positive endothelial cells, blank arrowhead: apoptotic pericyte. Bar: 50 μm.

combination of two genes were calculated according to their expression stability by the NormFinder program. The best fitting combination proved to be ß-actin with GAPDH.

The results of expression analysis showed slightly elevated levels of PTPIP51 (mean value 5.23±1.01) in the group of GBM when compared to low grade astrocytoma (mean value 4.62±1.49). 14-3-3ß expression in glioblastoma (mean value 3.42±1.10) was significantly higher than in grade II astrocytoma samples (mean value 0.88±2.74) (Fig. 9).

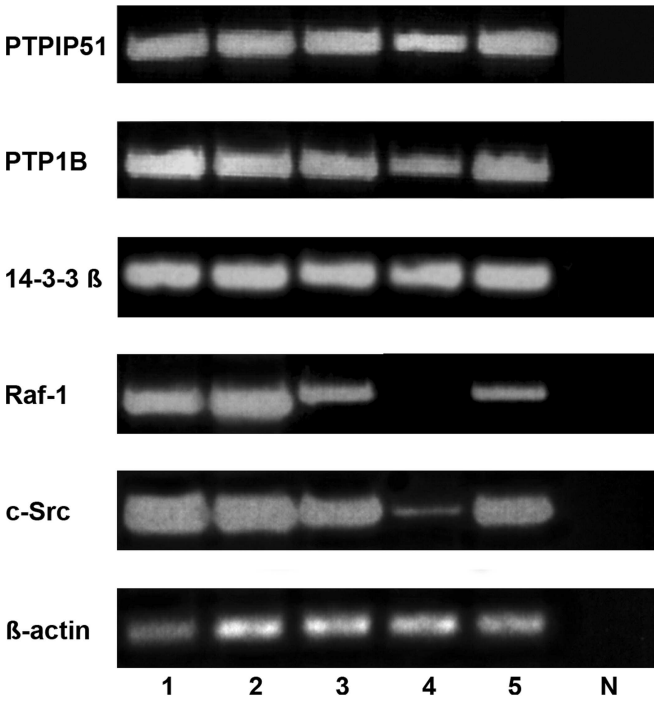

Fig. 8. Expression of PTPIP51 and its interaction partners as detected by reverse transcriptase-PCR in tissues of human glioblastoma. Qualitative reverse transcriptase-PCR was performed using primers specific to PTPIP51, PTP1B, Raf-1, c-Src and 14-3-3ß as given in Materials and Methods section. ß-actin was amplified as an internal positive control and probes lacking reverse transcriptase served as negative controls (N).

Discussion

Our results revealed elevated levels of PTPIP51 expression in GBM (grade IV glioma) samples when compared to low grade astrocytomas (grade II glioma), which correlated with the expression levels of 14-3-3ß. This is consistent with recent studies displaying a tumour grade dependent expression of two isoforms of 14-3-3ß and 14-3-3η in gliomas. Healthy cerebral tissue is completely lacking in both isoforms (Yang et al., 2009). The upregulation of 14-3-3 proteins seems to be associated with the reduced capacity of apoptosis, as antagonizing 14-3-3 or silencing its expression induces apoptosis in cultured glioma cells (Cao et al., 2010).

14-3-3ß and 14-3-3γ mediate the interaction of PTPIP51 and Raf-1, thereby modulating the activity of the MAPK-cascade (Lv et al., 2006; Yu et al., 2008; Stenzinger et al., 2009). The MAPK pathway plays an important role in cell migration and seems to be one of the main reasons for recurrences and poor prognosis of glioblastoma. It is considered that migrating tumour cells infiltrate the healthy tissue surrounding the glioblastoma and in this way can escape surgical extirpation and give rise to regrowth. With regard to these findings the interaction of PTPIP51 with 14-3-3ß, which was confirmed by the duolink proximity ligation assay, may mirror the role of PTPIP51 protein in migration and proliferation of GBM tumour cells.

A strong co-localization and interaction of PTPIP51 and 14-3-3ß was also found in all endothelial cells of GBM-typical glomerulum-like vessels of glioblastoma.

This interaction may contribute to the well known

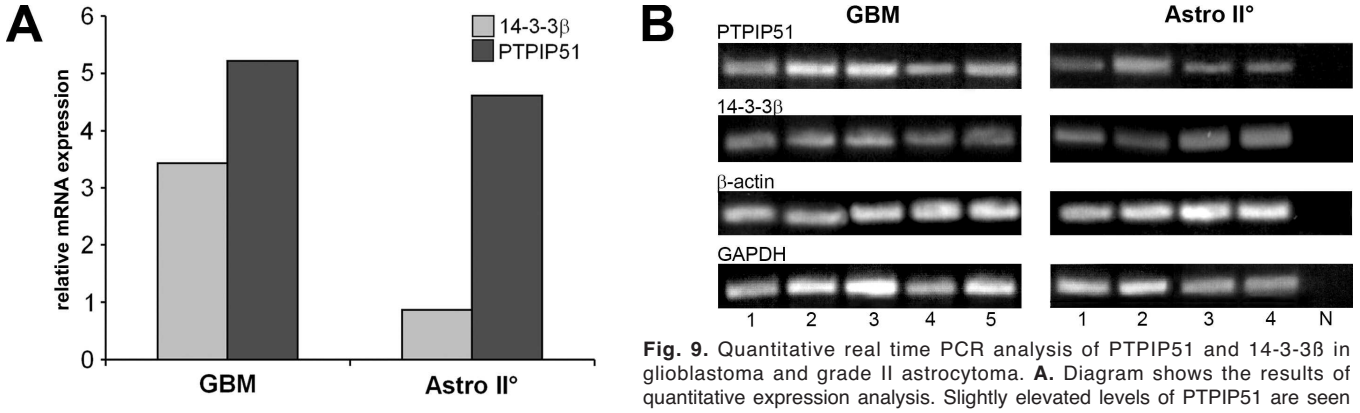

Fig. 9. Quantitative real time PCR analysis of PTPIP51 and 14-3-3ß in glioblastoma and grade II astrocytoma. **A.** Diagram shows the results of quantitative expression analysis. Slightly elevated levels of PTPIP51 are seen in the group of glioblastoma (GBM) when compared to low grade astrocytoma. 14-3-3ß expression in glioblastoma was significantly higher than in grade II astrocytoma samples. Amplification of ß-actin and GAPDH was used as a combination of reference genes. **B.** Gel: bands exclusively detecting mRNA with the expected amplification size with the primers used in 7A. Negative control (N).

high activation of the MAPK/Erk pathway via EGFR, resulting in dysfunction of cell cycle control and upregulation of proliferation in GBM.

The non-transmembrane Protein Tyrosine Phosphatase 1B (PTP1B), a known interacting partner of PTPIP51, is able to activate the MAPK cascade on c-Src and Ras level (Dubé et al., 2004; Dubé and Tremblay, 2004; Tonks and Muthuswamy, 2007; Zhao et al., 2008; Stenzinger et al., 2009). Reichardt and coworkers (2003) were unable to detect DNA amplification of PTP1B in human gliomas. However, in our study PTP1B expression was upregulated and highly co-localized with the PTPIP51 protein. The observed upregulation is consistent with the data reported by Akasaki and co-workers (2006), who also reported PTP1B to be overexpressed in gliomas. Furthermore, a direct *in situ* interaction of PTPIP51 and PTP1B in glioblastoma cells was corroborated by the duolink proximity ligation assay. These results underline the significance of our observations of upregulated PTPIP51 expression levels in glioblastomas.

PTP1B contributes to oncogenesis by the loss of tyrosine phosphorylation of key signalling proteins or by up-regulation of two growth-promoting pathways (Arias-Romero et al., 2009). In human mammary cells PTP1B links an important oncogenic receptor tyrosine kinase, namely ErbB2, to signalling pathways that promote aberrant cell division and survival by activation of Src and inducing a Src-dependent transformed phenotype. It deactivates the Ras/MAPK pathway inhibitor (Tonks and Muthuswamy, 2007).

C-Src mediates the phosphorylation of EGFR, thereby promoting tumour progression (Tice et al., 1999). The ultimate cellular response to the activation of EGFR signalling cascade via MAPK pathway is DNA synthesis and cell division (Halatsch et al., 2004). In our samples PTPIP51 and EGFR were partly co-localized, suggesting a synergistic effect on cell proliferation, migration and oncogenic transformation. This may be exerted by sharing the same final signalling pathway, PTPIP51 via 14-3-3ß interaction with Raf-1 and EGFR activating the Ras/Raf/MAPK/ERK pathway. Compared to secondary GBM, developed by progression from lower grade gliomas, EGFR gene amplification has been shown to be five times higher in primary glioblastoma, which leads to overexpression in 40% of GBM (Karpel-Massler et al., 2009). Besides this EGFR overexpression, EGFR is expressed as the mutated EGFRvIII (epidermal growth factor receptor variant III) form of the receptor in 20% of GBM cases (Jutten et al., 2009). This constitutively active mutant form of the EGFR, which is commonly expressed in glioblastoma, is also detected in a number of epithelial cancers (Yoshimoto et al., 2008; Hama et al., 2009) also known to express high concentrations of PTPIP51, e.g. non melanoma skin cancer, prostate cancer (Koch et al., 2008; 2009b) and breast cancer. EGFR signalling cascade via MAPK pathway is modulated by PTP1B through c-Src and by 14-3-3ß through Raf-1 (Yu et al., 2008), both interaction partners of PTPIP51. This *in situ* interaction in GBM was substantiated in our study by duolink proximity ligation assay (Gajadhar and Guha, 2010).

Glial malignant transformation might be correlated to the status of PTPIP51 gene promotor methylation, since high grade gliomas (GBM) also presented a higher mRNA expression of PTPIP51 in comparison to low grade gliomas (grade II astrocytoma).

To sum up, in neuroepithelial tumours, PTPIP51 expression increases with the grade of malignancy and PTPIP51 interacts *in situ* with 14-3-3ß and PTP1B. The data presented in this study suggest an important role of PTPIP51 in glioblastoma formation.

Acknowledgements We are grateful to Mrs. K. Michael (Institute of Anatomy and Cell Biology, Giessen) for help with the design of the figures and to Mrs. A. Peters (Department of Neurosurgery, Giessen) for help in providing the glioblastoma samples. The excellent techncial assistance of Mrs. A. Erkel, Mrs. B. Fröhlich (Department of Urology and Pediatric Urology, Giessen), Mrs. A. zur Mühlen (Institute of Neuropathology, Bonn) and Mrs. C. Tag (Institute of Anatomy and Cell Biology, Giessen) is gratefully acknowledged.

References

Akasaki Y., Liu G., Matundan H.H., Ng H., Yuan X., Zeng Z., Black K.L. and Yu J.S. (2006). A peroxisome proliferator-activated receptor-gamma agonist, troglitazone, facilitates caspase-8 and -9 activities by increasing the enzymatic activity of protein-tyrosine phosphatase-1B on human glioma cells. J. Biol. Chem. 281, 6165-6174.

Arias-Romero L.E., Saha S., Villamar-Cruz O., Yip S.C., Ethier S.P., Zhang Z.Y. and Chernoff J. (2009). Activation of Src by protein tyrosine phosphatase 1B is required for ErbB2 transformation of human breast epithelial cells. Cancer Res. 69, 4582-4588.

Cao L., Cao W., Zhang W., Lin H., Yang X., Zhen H., Cheng J., Dong W., Huo J. and Zhang X. (2008). Identification of 14-3-3 protein isoforms in human astrocytoma by immunohistochemistry. Neurosci. Lett. 432, 94-99.

Cao W., Yang X., Zhou J., Teng Z., Cao L., Zhang X. and Fei Z. (2010). Targeting 14-3-3 protein, difopein induces apoptosis of human glioma cells and suppresses tumor growth in mice. Apoptosis 15, 230-241.

Dubé N. and Tremblay M.L. (2004). Beyond the metabolic function of PTP1B. Cell Cycle. 3, 550-553.

Dubé N., Cheng A. and Tremblay M.L. (2004). The role of protein tyrosine phosphatase 1B in Ras signalling. Proc. Nat. Acad. Sci. USA 101, 1834-1839.

Ewing R.M., Chu P., Elisma F., Li H., Taylor P., Climie S., McBroom-Cerajewski L., Robinson M.D., O'Connor L., Li M., Taylor R., Dharsee M., Ho Y., Heilbut A., Moore L., Zhang S., Ornatsky O., Bukhman Y.V., Ethier M., Sheng Y., Vasilescu J., Abu-Farha M., Lambert J.P., Duewel H.S., Stewart I.I., Kuehl B., Hogue K., Colwill K., Gladwish K., Muskat B., Kinach R., Adams S.L., Moran M.F., Morin G.B., Topaloglou T. and Figeys D. (2007). Large-scale mapping of human protein-protein interactions by mass spectrometry. Mol. Syst. Biol. 3, 89.

Gajadhar A. and Guha A. (2010). A proximity ligation assay using transiently transfected, epitope-tagged proteins: application for *in*

situ detection of dimerized receptor tyrosine kinases. Biotechniques. 48, 145-152

Halatsch M.E., Gehrke E.E., Vougioukas V.I., Bötefür I.C., A-Borhani F., Efferth T., Gebhart E., Domhof S., Schmidt U. and Buchfelder M. (2004). Inverse correlation of epidermal growth factor receptor messenger RNA induction and suppression of anchorage-independent growth by OSI-774, an epidermal growth factor receptor tyrosine kinase inhibitor, in glioblastoma multiforme cell lines. J. Neurosurg. 100, 523-533.

Hama T., Yuza Y., Saito Y., Ouchi J., Kondo S., Okabe M., Yamada H., Kato T., Moriyama H., Kurihara S. and Urashima M. (2009). Prognostic significance of epidermal growth factor receptor phosphorylation and mutation in head and neck squamous cell carcinoma. Oncologist 14, 900-908.

Jin J., Smith F.D., Stark C., Wells C.D., Fawcett J.P., Kulkarni S., Metalnikov P., O'Donnell P., Taylor P., Taylor L., Zougman A., Woodgett J.R., Langeberg L.K., Scott J.D. and Pawson T. (2004). Proteomic, functional, and domain-based analysis of *in vivo* 14-3-3 binding proteins involved in cytoskeletal regulation and cellular organization. Curr. Biol. 14, 1436-1450.

Jutten B., Dubois L., Li Y., Aerts H., Wouters B.G., Lambin P., Theys J. and Lammering G. (2009) Binding of cetuximab to the EGFRvIII deletion mutant and its biological consequences in malignant glioma cells. Radiother. Oncol. 92, 393-398.

Karpel-Massler G., Schmidt U., Unterberg A. and Halatsch M.E. (2009). Therapeutic inhibition of the epidermal growth factor receptor in high-grade gliomas: where do we stand? Mol. Cancer. Res. 7, 1000-1012.

Khan M.K., Hunter G.K., Vogelbaum M., Suh J.H. and Chao S.T. (2009). Evidence-based adjuvant therapy for gliomas: current concepts and newer developments. Indian J. Cancer 46, 96-107.

Koch P., Stenzinger A., Viard M., Märker D., Mayser P., Nilles M., Schreiner D., Steger K. and Wimmer M. (2008). The novel protein PTPIP51 is expressed in human keratinocyte carcinomas and their surrounding stroma. J. Cell. Mol. Med. 12, 2083-2095.

Koch P., Viard M., Stenzinger A., Brobeil A., Tag C., Steger K. and Wimmer M. (2009a). Expression profile of PTPIP51 in mouse brain. J. Comp. Neurol. 517, 892-905.

Koch P., Petri M., Paradowska A., Stenzinger A., Sturm K., Steger K. and Wimmer M. (2009b). PTPIP51 mRNA and protein expression in tissue microarrays and promoter methylation of benign prostate hyperplasia and prostate carcinoma. Prostate 69, 1751-1762.

Lopez-Gines C., Gil-Benso R., Benito R., Mata M., Pereda J., Sastre J., Roldan P., Gonzalez-Darder J. and Cerdá-Nicolás M. (2008). The activation of ERK1/2 MAP kinases in glioblastoma pathobiology and its relationship with EGFR amplification. Neuropathology 28, 507-515.

Lv B.E., Yu C.E., Chen Y.Y., Lu Y., Guo J.H., Song Q.S., Ma D.L., Shi T.P. and Wang L. (2006). Protein tyrosine phophatase interacting interacting protein 51 (PTPIP51) is a novel mitochondria protein with an N-terminal mitochondrial targeting sequence and induces apoptosis. Apoptosis 11, 1489-1501.

McLendon R.E., Turner K., Perkinson K. and Rich J. (2007). Second messenger systems in human gliomas. Arch. Pathol. Lab. Med. 131, 1585-1590.

Reichardt W., Jung V., Brunner C., Klein A., Wemmert S., Romeike B.F., Zang K.D. and Urbschat S. (2003). The putative serine/threonine kinase gene STK15 on chromosome 20q13.2 is amplified in human gliomas. Oncol. Rep. 10, 1275-1279.

Stenzinger A., Kajosch T., Tag C., Porsche A., Welte I., Hofer H.W., Steger K. and Wimmer M. (2005). The novel protein PTPIP51 exhibits tissue- and cell-specific expression. Histochem. Cell. Biol. 123, 19-28.

Stenzinger A., Schreiner D., Koch P., Hofer H.W. and Wimmer M. (2009). Cell- and molecular biology of the novel protein tyrosine phosphatase interacting protein 51. Int. Rev. Cell. Mol. Biol. 275, 183-246.

Tice D.A., Biscardi J.S., Nickles A.L. and Parsons S.J. (1999). Mechanism of biological synergy between cellular Src and epidermal growth factor receptor. Proc. Nat. Acad. Sci. USA 96, 1415-1420.

Tonks N.K. and Muthuswamy S.K. (2007). A brake becomes an accelerator: PTP1B - a new therapeutic target for breast cancer. Cancer Cell 11, 214-216.

Yang X., Cao W., Lin H., Zhang W., Lin W., Cao L., Zhen H., Huo J. and Zhang X. (2009). Isoform-specific expression of 14-3-3 proteins in human astrocytoma. J. Neurol. Sci. 276, 54-59.

Yoshimoto K., Dang J., Zhu S., Nathanson D., Huang T., Dumont R., Seligson D.B., Yong W.H., Xiong Z., Rao N., Winther H., Chakravarti A., Bigner D.D., Mellinghoff I.K., Horvath S., Cavenee W.K., Cloughesy T.F. and Mischel P.S. (2008). Development of a real-time RT-PCR assay for detecting EGFRvIII in glioblastoma samples. Clin. Cancer Res. 14, 488-493.

Yu C., Han W., Shi T., Lv B., He Q., Zhang Y., Li T., Zhang Y., Song Q., Wang L. and Ma D. (2008). PTPIP51, a novel 14-3-3 binding protein, regulates cell morphology and motility via Raf-ERK pathway. Cell. Signal. 20, 2208-2220.

Zhao Y., Xiao A., Dipierro C.G., Abdel-Fattah R., Amos S., Redpath G.T., Carpenter J.E., Pieper R.O. and Hussaini, I.M. (2008). H-Ras increases urokinase expression and cell invasion in genetically modified human astrocytes through Ras/Raf/MEK signalling pathway. Glia 56, 917-924.

Accepted June 15, 2011